Effects of ethylene glycol addition on the properties of Ru/Al_2O_3 catalyst prepared by sol–gel method

J.C. Yang and Y.G. Shul

Department of Chemical Engineering, Yonsei University, Sinchondong Sudaemungu, 120-749, Seoul, Korea

Received 16 June 1995; accepted 31 August 1995

Ru/Al_2O_3 catalysts were prepared by sol–gel method with an organic additive (ethylene glycol). The effect of the addition of ethylene glycol on the properties of Ru/Al_2O_3 was characterized by BET, XRD, EXAFS, and TGA/DTA. Ethylene glycol was effective to promote the phase transition of α-Al_2O_3 even at 800°C calcination with high surface area. This finding is ascribed to the modified structure of aluminum alkoxide by ethylene glycol addition in the solution state. Ethylene glycol is also effective to get small particles of ruthenium after the reduction at 500°C. The EXAFS and UV-Vis spectra of Ru complex revealed that the coordination structure of Ru depended on the additive used. The ethylene glycol sol prefers to form octahedral Ru complex. This Ru complex in alumina matrix is stable up to 200°C and forms small Ru oxide particles even at 300°C calcination. This suggests that ethylene glycol coordinates to the Ru complex as well as to aluminum ion in the initial state, which is important to control the final properties of the Ru/Al_2O_3 catalyst.

Keywords: sol–gel; Ru/Al_2O_3; ethylene glycol; characterization; chelating agent

1. Introduction

Ruthenium supported catalysts have been widely used in Fischer–Tropsch synthesis [1], hydrogenolysis of paraffins and olefins [2]. In these reactions, catalytic activity and selectivity to products are greatly affected by the dispersion of Ru and the nature of support such as surface area, pore structure and thermal stability [3]. It is well-known that the dispersion and nature of support are strongly dependent on the method of catalyst preparation employed [4].

Recently, the sol–gel method that starts from homogeneous alkoxide solution has been proposed. The sol–gel method starts with the molecular precursor of the support material and active metal. A greater degree of control over the catalyst preparation can be achieved in comparison to the traditional preparation method [5]. The advantages of the sol–gel method compared with the conventional impregnation method are as follows: (a) homogeneity and high purity, (b) high BET surface area and well-defined pore control and (c) easy control of active metal particle size. Lopez et al. prepared Ru/SiO_2 catalyst by the sol–gel method, whereby most of ruthenium particles were incorporated in the silica matrix. This catalyst allows better selectivity and greater resistance to coke formation and deactivation in benzene hydrogenation reaction than the catalyst prepared by the traditional impregnation method, which is attributed to structural differences in the prepared catalysts [6–9]. Balakrishman obtained very porous and well-dispersed Pt/Al_2O_3 by controlling the preparation parameters like H_2O/alkoxide ratio in sol–gel preparation [10].

The chemical modification of metal alkoxides with chelating agents such as beta-diketones is known to be very effective for the control of reactivities and condensation process of metal alkoxides [11]. The structural modification of Al alkoxide by ethylacetoacetate has been reported to yield very fine and porous Al_2O_3 [12]. Inoui et al. prepared the bohemite in which ethylene glycol moiety was incorporated between alumina layers through covalent bonding by thermal decomposition of aluminum isopropoxide in inert organic solvent at 250–300°C [13,14]. Mizukami et al. investigated the effects of organic additives on the Al_2O_3 gel by sol–gel method, and the thermal stability and pore structure of the prepared Al_2O_3 appeared to be greatly affected by the complexing ability of the organic solvent [15]. Shul et al. found hexylene glycol was an effective organic additive to lower the phase transition temperature of rutile from the alkoxide derived TiO_2 gel in oxygen steam treatment at 300°C [16]. These studies denote the importance of chelating agents which affect the thermal stability and morphology of prepared gel in sol–gel transformation.

In this study, the effects of ethylene glycol addition on the properties of Ru/Al_2O_3 catalysts were discussed. The changes of coordination state around Ru, from initial solution to final reduced metal state, were characterized by means of BET, XRD, TGA/DTA, ^{13}C-NMR, and EXAFS.

2. Experimental

2.1. Preparation of 5 wt% Ru/Al_2O_3 catalyst

The schematic preparation procedure of Ru/Al_2O_3 by the sol–gel method was as follows (fig. 1): 12.3 g of

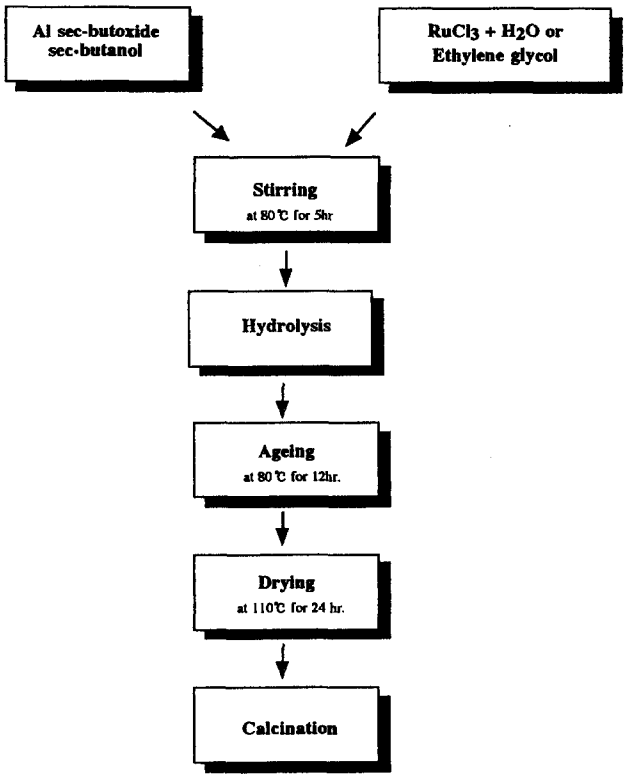

Fig. 1. The preparation procedure of Ru/Al_2O_3 catalyst by the sol–gel method.

aluminum sec-butoxide ($Al(OC_4H_9)_3$, Aldrich) was diluted with 14.824 g of sec-butanol (C_4H_9OH, Fisher Sci. Co.), under reflux at 80°C, and 0.275 g of ruthenium chloride ($RuCl_3$, Janssen of Chemica) was dissolved in 16 g of ethylene glycol ($OHCH_2CH_2OH$, Yakuri Pure Chemical) or 6 g of deionized H_2O, respectively. The Al alkoxide and $RuCl_3$ solution were mixed and stirred at 80°C for 5 h. The Ru/Al_2O_3 gel was prepared by hydrolyzing the mixed sol with 0.9 g of deionized H_2O at 80°C. The prepared gel was dried at 110°C for 24 h and calcined at 200, 300, 500°C for 7 h, respectively.

The γ-Al_2O_3 (Strem Chem. Inc.) was impregnated with aqueous $RuCl_3$ solution. The sample was dried at 110°C and calcined at 200, 300, 500°C, respectively.

In the following, EG-T, and W-T identify the catalysts prepared by using different solvents in the sol–gel method; EG and W denote the ethylene glycol and H_2O added samples, and T identifies the calcination temperature. Im-T denotes the catalyst prepared by the impregnation method. For example, the ethylene glycol added Ru/Al_2O_3 calcined at 300°C is denoted by EG-300.

2.2. XRD measurement

X-ray diffraction patterns were measured with an X-ray diffractometer (D-max3, Rigaku) employing Cu-Kα radiation and a nickel filter. The scanning was done at the range of $2\theta = 20$–$70°$.

2.3. Surface area measurement

The surface of Ru/Al_2O_3 was measured by a continuous one-point BET method [17]. The samples were packed in a Pyrex reactor and then calcined at 500°C for 2 h. The nitrogen adsorption was performed at liquid nitrogen temperature and the nitrogen effluent was monitored by a thermal conductivity detector.

2.4. EXAFS measurement

The samples were characterized by EXAFS spectroscopy using synchrotron radiation at the Photon Factory (Japan). The storage ring was operated with an electron energy of 2.5 GeV and a current between 250 and 300 mA. BL-10B was used as beam line with the Si(311) monochromator in the transmission mode. The EXAFS measurements were done at the Ru K-edge (22110 eV). For good signal to noise ratio, samples were pressed into self-supporting wafers. The reduction was conducted with hydrogen in a glass cell which was sealed off with a flame in hydrogen atmosphere. The solution samples were contained in a glass tube holder, through which X-ray passed, and the thickness of the holder was adjusted in order to obtain optimal signals. The k^3-weighted chi spectra were Fourier transformed from k to R space using Hanning window functions ($\Delta k = 2.6$–13.6 Å^{-1}). Curve fitting was carried out by the conventional fitting method suggested by Teo [18]. RuO_2, $RuCl_3$ and bulk Ru metal were used as reference compounds for amplitude and phase function calculations.

2.5. Thermal analysis

Thermal gravimetry and thermal differential analysis were carried out on a Shimadzu TG-70 instrument with a heating rate of 10°C/min under a nitrogen flow of 50 ml/min.

3. Results

3.1. Specific surface area of Ru/Al_2O_3

Fig. 2 shows the BET surface areas of Ru/Al_2O_3 samples calcined at 500 and 800°C for 7 h. After calcination at 500°C, the surface area of the EG-500 sample prepared by the sol–gel method was 290 m^2/g. Whereas, in the impregnated sample, the surface area of Im-500 was 245 m^2/g. At 800°C calcination, the surface area of EG-800 was 237 m^2/g and the surface areas of W-800 and Im-800 decreased to 190 and 185 m^2/g, respectively.

Maeda et al. reported that high surface area aluminas were obtained by using complexing agents such as hexylene glycol by sol–gel process [33,34]. Our BET surface area results show that ethylene glycol was also an effec-

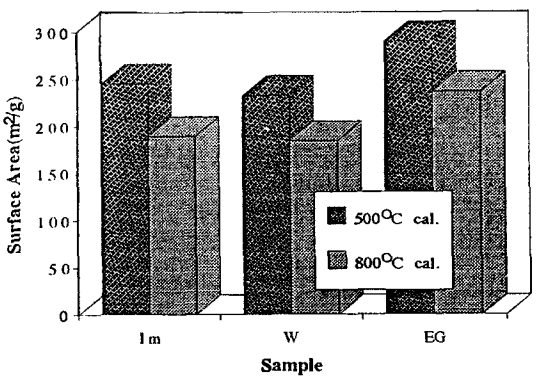

Fig. 2. BET surface area of Ru/Al_2O_3 catalysts calcined at 500°C and 800°C; Im: Ru impregnated on γ-Al_2O_3, W: sol–gel Ru/Al_2O_3 (H_2O solvent), and EG: sol–gel Ru/Al_2O_3 (ethylene glycol solvent).

tive complexing agent to maintain high surface area after 800°C calcination.

3.2. The phase transition of Ru/Al_2O_3

Fig. 3 shows the X-ray diffraction patterns of Ru/Al_2O_3 calcined at 700°C. The characteristic peak of α-Al_2O_3 phase at $2\theta = 43.25°$ was observed in the EG-700 sample. By contrast, in the samples of W-700 and Im-700, the α-Al_2O_3 phase peak was not observed, instead, the γ-Al_2O_3 phase appeared after 700°C calcination. In addition, the intensity of RuO_2 peak ($2\theta = 28.15°$) in the W-700 sample was stronger than that of the EG-700 sample, which denotes the large RuO_2 particles were formed in the W-700 sample at 700°C calcination.

Fig. 4 shows the X-ray diffraction patterns of Ru/Al_2O_3 calcined at 800°C. The α-Al_2O_3 peak was markedly observed in EG-800 and the diffraction patterns were sharp, indicating the development of α-phase at 800°C calcination. By contrast, γ-phase was observed in Im-800, and mixed phases, γ and δ with small amount of α phase, were shown in the XRD pattern of W-800. From these patterns, the degree of phase transition to α-phase are in the order EG-800 > W-800 > Im-800.

It is reported that the phase transition temperature of α-Al_2O_3 normally occurs in the range of 1150–1200°C with remarkable decrease of surface area due to the sintering of intermediate phase during the course of phase transformation at high temperature calcination [19]. However, by adding ethylene glycol to Ru/Al_2O_3 sol, the phase transition temperature of the α-phase lowered more than 450–350°C in comparison with the conventional preparation of Al_2O_3. It suggests that the stabilized α-phase formed at 800°C prevents the sintering of alumina and maintains high surface area, as shown in fig. 2 at high temperature calcination.

3.3. Thermal analysis of Ru/Al_2O_3

Fig. 5 shows the thermal analysis results of EG-gel. Three endothermic peaks and two exothermic peaks are shown in the DTA profile of EG-gel. Mizukami studied the Al_2O_3 phase transition prepared by the sol–gel method with a complexing agent. The two endothermic peaks of DTA spectra at 373 and 723 K assigned to the desorption of physically adsorbed water molecule and elimination of H_2O from adjacent hydroxyl groups between bohemite layers were shown, respectively [15]. The exothermic peaks corresponding to the decomposition of organic molecules in DTA profile were strongly affected by the strength of the complexing abilities of the organic chelating agent in the dry gel [15]. Based on this study, the endothermic peaks below 200 and 420°C can be assigned to the desorption of physically adsorbed water and the elimination of chemically adsorbed H_2O, respectively. Two exothermic peaks at ca. 390 and 440°C might be assigned to the decomposition of residual alkoxide (alkyl group) and ethylene glycol. A broad

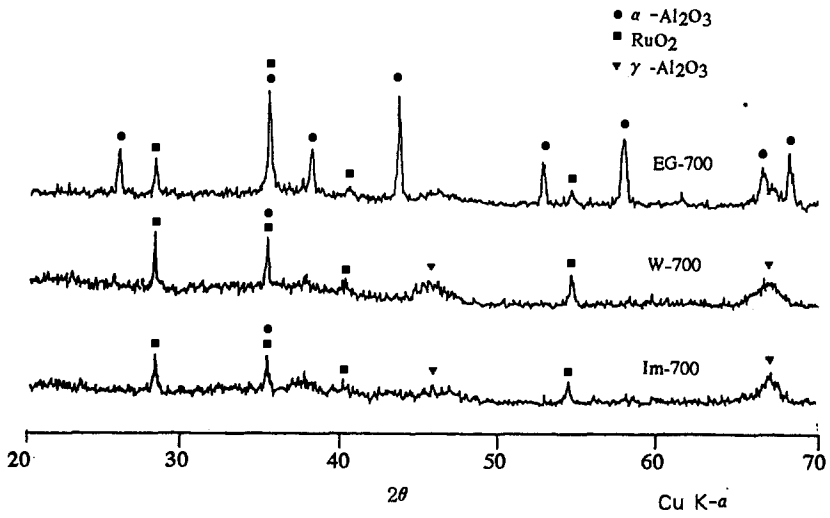

Fig. 3. XRD patterns of Ru/Al_2O_3 catalysts calcined at 700°C.

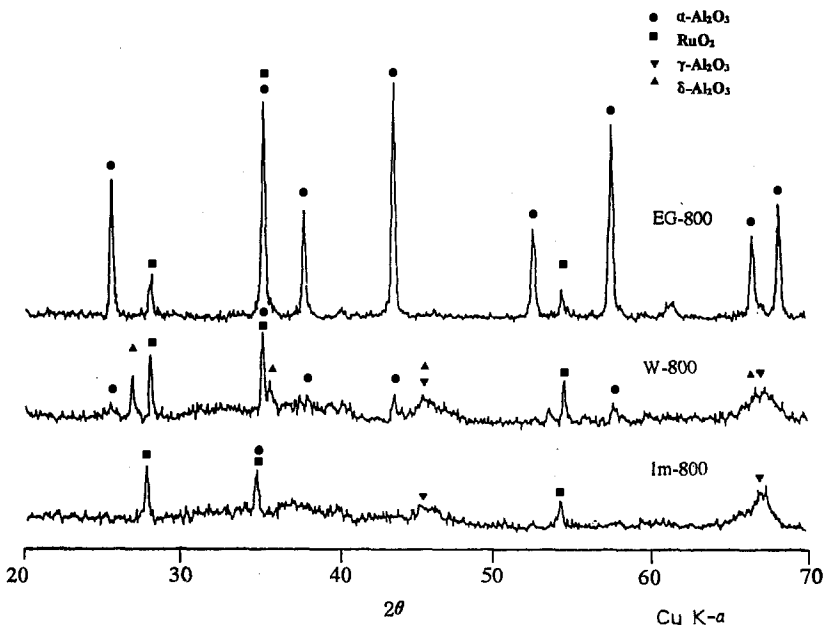

Fig. 4. XRD patterns of Ru/Al_2O_3 catalysts calcined at 800°C.

exothermic peak which corresponds to phase transition from amorphous to α-phase was observed between 440 and 800°C.The DTA data are well consistent with the phase transition behaviors of Al_2O_3 observed in XRD spectra.

The ^{13}C-NMR spectra of ethylene glycol solution, EG-200 and EG-300 are shown in fig. 6. The peak at 62.62 ppm which corresponds to carbon of ethylene glycol is shown in ^{13}C-NMR spectra of ethylene glycol solution. In the EG-200 sample, three peaks are observed at 19.67, 61.93, and 181.66 ppm. Tohji et al. reported that the peaks of ^{13}C-NMR spectra caused by ethylene glycol and ethylene glycol coordinated to Ni atom appeared at ca. 60 ppm and ca. 25 ppm, respectively [21,29]. Based on this study, the peaks at 61.93 and 19.67 ppm can be assigned to the carbon atom of ethylene glycol and ethylene glycol coordinated to ruthenium, respectively. The other peak at 181.66 ppm may come from the signal of carbon containing ethylene glycol–aluminum interaction because this is the only possible carbon signal in this reaction mixture. As the calcination temperature increases to 300°C, no peaks were shown in the spectra, which implies the destruction of ethylene glycol bondings with Ru or Al below 300°C.

From the TGA/DTA and ^{13}C-NMR results, it may be concluded that ethylene glycol should have strong

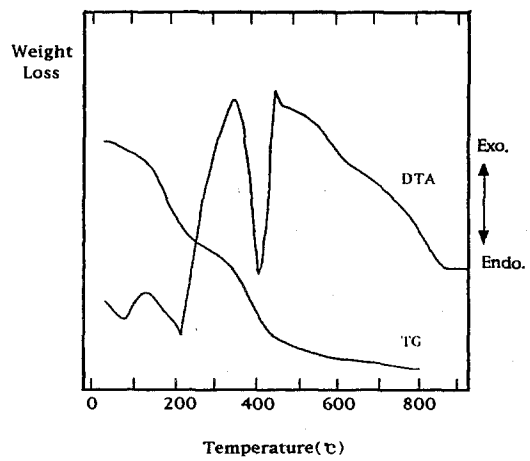

Fig. 5. TGA and DTA curves of EG-gel.

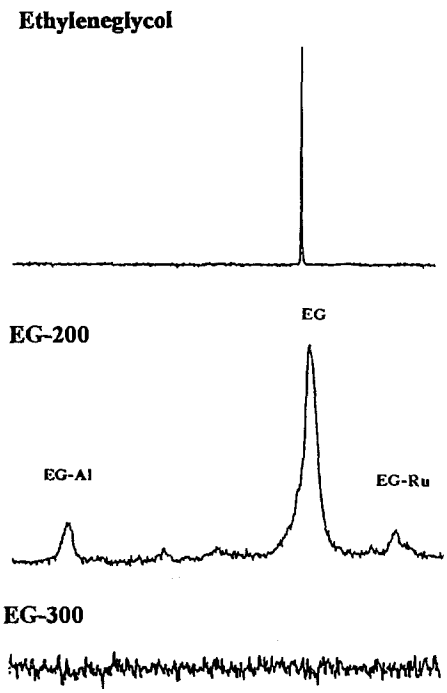

Fig. 6. ^{13}C-NMR spectra of ethylene glycol, EG-200 and EG-300 catalysts.

bonds with both aluminum and ruthenium in the initial solution state, and after forming an amorphous powder those bonds are still maintained up to 200°C calcination and start to decompose above 300°C calcination.

3.4. Coordination state of Ru in solution

EXAFS is a sufficient surface characterization method to determine the local structure around one atom. To characterize the coordination state of Ru in $RuCl_3$ solution using different solvents (ethylene glycol and H_2O), the EXAFS spectra were measured at the Ru K-edge in synchrotron radiation. Fig. 7 shows the Fourier transform and curve fitting results of $RuCl_3$ solution with ethylene glycol and H_2O solvent. In the Fourier transform of EG-sol (fig. 7A) without phase shift correction, one main peak is apparently shown in radial structure function around 2.0 Å. As well as a main peak around 1.9 Å, the second shell interaction around 3.0 Å is shown in EXAFS spectra of W-sol (fig. 7C). The first peak below 2.0 Å can be attributed to the combination of Ru–O and Ru–Cl interaction, which was confirmed by the two-shell model (Ru–O + Ru–Cl) curve fitting results [22,23]. The two-shell model composed of Ru–O and Ru–Cl gave a good curve-fitting result as shown in fig. 7B and 7D. The second shell interaction around 3.0 Å which corresponds to Ru–O and Ru–Ru is shown in radial structure function of $RuCl_3$ aqueous solution [36].

The EXAFS fitting results of $RuCl_3$ solution are shown in table 1. In the fitting results of EG-sol, Ru–O and Ru–Cl bonds existed at 2.08 and 2.36 Å, respectively. The coordination numbers of Ru–O and Ru–Cl bonds are 4.2 and 2.2, respectively. Therefore, EG-sol should have octahedral Ru complex in the solution state, where the Ru–O bonds should come from the interaction of bidentate ethylene glycol coordinated to the Ru atom. In $RuCl_3$ aqueous solution, the Ru–O bond is observed at 1.75 Å with a coordination number of 1.2, and the Ru–Cl distance was 2.34 Å with a coordination number of 2.7. This means that ruthenium might have four coordinated structure in W-sol. From those fitting results, the Ru–O bond length of W-sol is 0.25 Å shorter than that of EG-sol. Generally, the Ru–O bond can be found to be 1.9–2.1 Å [22,23,36,26]. From X-ray crystallography data [37], the octahedral RuO_2 had six Ru–O

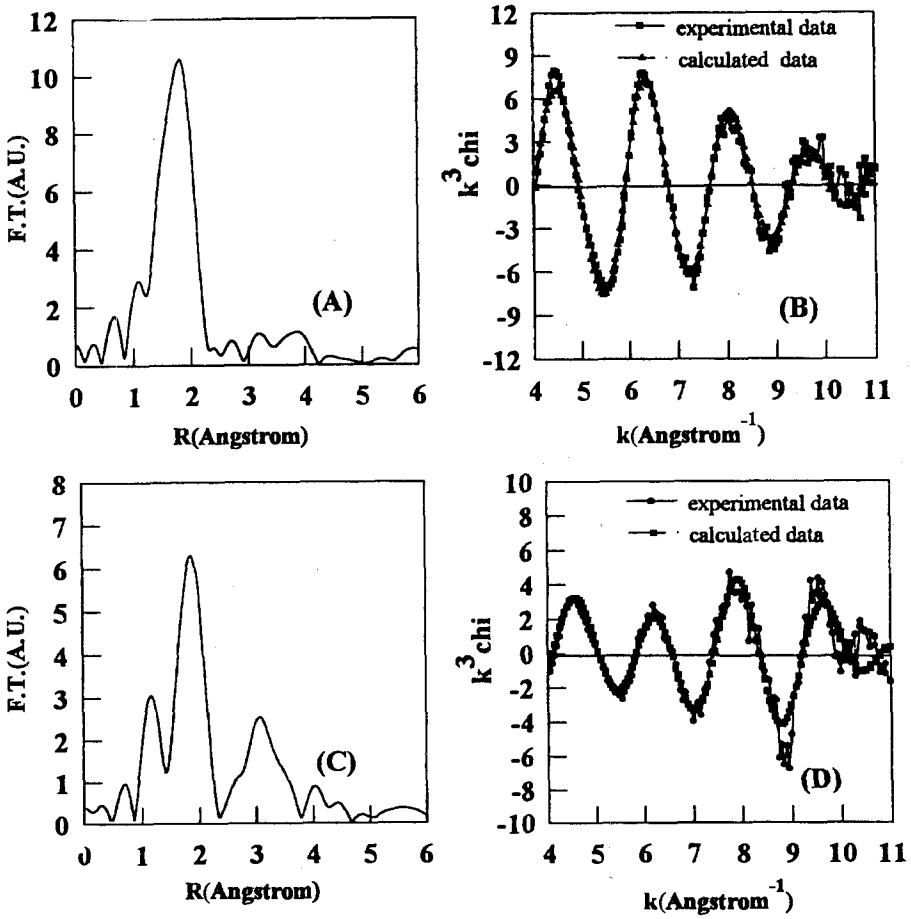

Fig. 7. (A) Fourier transform of the k^3-weighted χ data of EG-sol (without phase shift corrected), (B) k^3- weighted χ data and best fit result of EG-sol, (C) Fourier transform of k^3-weighted χ data of W-sol (without phase shift corrected), and (D) k^3-weighted χ data and best fit result of W-sol.

Table 1
Best fit values of the EXAFS spectrum of $RuCl_3$ solutions at the Ru K-edge [a]

Sample	Back scatterer	N	R (Å)	$\Delta\sigma^2$ (Å^2)
EG-sol	O	4.2 ± 0.5	2.09 ± 0.03	$0.005 \pm 20\%$
	Cl	2.2 ± 0.3	2.36 ± 0.02	$0.002 \pm 20\%$
W-sol	O	1.2 ± 0.1	1.75 ± 0.01	$0.001 \pm 10\%$
	Cl	2.7 ± 0.3	2.34 ± 0.01	$0.005 \pm 15\%$

[a] N is the coordination number (for the absorber scatter), R is the interatomic distance, and $\Delta\sigma^2$ is the difference between σ^2 values of the sample and the reference.

bond lengths at 1.917 Å (4Ru–O) and 1.999 Å (2Ru–O). In contrast, the Ru–O bond can be found at 1.705 Å in tetrahedral RuO_4. The X-ray crystallography results imply that the differences of Ru–O bond length can be attributed to the structural difference around Ru (octahedral and tetrahedral). The different metal–oxygen bond lengths (1.6 and 2.0 Å) have also been suggested by EXAFS results of Cr ions, which exhibit the two oxidation states in mixed solvent system [38].

Fig. 8 shows the UV-Vis spectra of $RuCl_3$ solution using different solvents (H_2O and ethylene glycol). The UV spectra of EG-sol contain absorption peaks at ca. 220, 270 and 410 nm. The UV spectrum of EG-sol is analogous to the UV spectra of octahedral Ru(III) complex ($Ru(H_2O)_6^{3+}$) which has a strong absorption peak at ca. 220 nm. The strongest absorption peak of 220 nm might be assigned to a ligand to metal charge-transfer transition of Ru(III) complex [24,25]. While, in W-sol, the peak at 220 nm disappeared, instead, the peak at 382 nm was shown in UV-Vis data of W-sol. In W-sol, the absorption band corresponds to the charge-transfer transition appearing at 220 nm for EG-sol shifted to the lower energy region. In our preparation condition of W-sol (pH = 4.5), the Ru complex seems to be unstable under high pH condition [25]. Thus, a different configuration of the Ru complex compared with EG-sol and $Ru(H_2O)_6^{3+}$ could be formed in W-sol.

When we consider the data from EXAFS coordination numbers and UV-Vis results, we may conclude that the structure of Ru complex in solution state depends upon the solvents (ethylene glycol or H_2O). Namely, the EG-sol prefers to form the octahedral Ru complex, and W-sol possibly prefers to form the tetrahedral structure in solution state.

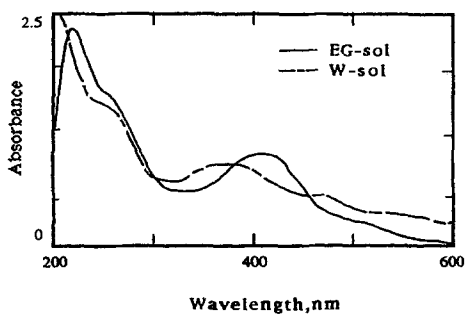

Fig. 8. UV-Vis spectra of $RuCl_3$ solutions.

3.5. Calcined and reduced Ru/Al_2O_3

Fig. 9 shows the Fourier transform of EXAFS spectra of Ru/Al_2O_3 after 300°C calcination in air atmosphere. In EXAFS results, the ruthenium oxide begins to appear in radial structure function of the sample after 300°C heat treatment. In the Fourier transforms of Ru/Al_2O_3 catalysts calcined at 300°C, the Ru–O and Ru–Ru interactions from ruthenium oxide are observed at ca. 3.4 Å. From the fitting results (table 2), the Ru–O and Ru–Ru coordination numbers of EG-300 (CN of Ru–O = 3.0, Ru–Ru = 0.9) are smaller than those of the W-300 sample (CN of Ru–O = 4, Ru–Ru = 1.0), which means the EG-300 has smaller oxide particles than the W-300 sample.

The fitting results of Ru/Al_2O_3 calcined at 500°C and reduced at 500°C are shown in table 3. The Ru–Ru coordination number of EG-500 is smaller than that of other catalysts. The coordination number of Im-5 is 11.4, which denotes that large Ru metal particles are formed in impregnation method. Judging from the coordination number of Ru, the sol–gel Ru/Al_2O_3 with ethylene glycol should have the smallest particles of Ru in prepared catalysts.

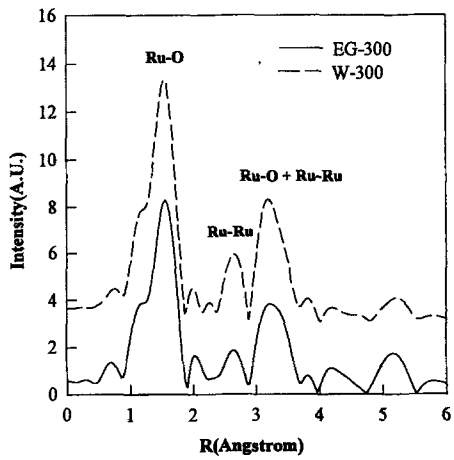

Fig. 9. Fourier transform of EXAFS spectra of Ru/Al_2O_3 catalysts calcined at 300°C (without phase shift correction).

Table 2
Best fit values of the EXAFS spectrum of Ru/Al_2O_3 catalysts calcined at 300°C [a]

Sample	Shell	N	R (Å)	$\Delta\sigma^2$ (Å^2)
EG-300	Ru–O	2.3 ± 0.2	1.92 ± 0.02	0.008 ± 15%
	Ru–O	3.0 ± 0.2	1.99 ± 0.02	0.003 ± 18%
	Ru–Ru	0.2 ± 0.1	3.02 ± 0.03	0.006 ± 15%
	Ru–O	3.0 ± 0.2	3.37 ± 0.02	0.001 ± 15%
	Ru–Ru	0.9 ± 0.1	3.52 ± 0.02	−0.0005 ± 15%
W-300	Ru–O	2.4 ± 0.3	1.91 ± 0.03	0.007 ± 15%
	Ru–O	2.7 ± 0.1	1.99 ± 0.01	0.002 ± 14%
	Ru–Ru	1.6 ± 0.2	3.05 ± 0.01	0.008 ± 13%
	Ru–O	4.0 ± 0.3	3.32 ± 0.02	0.003 ± 15%
	Ru–Ru	1.0 ± 0.1	3.57 ± 0.02	−0.0001 ± 15%

[a] N is the coordination number (for the absorber scatter), R is the interatomic distance, and $\Delta\sigma^2$ is the difference between σ^2 values of the sample and the reference.

4. Discussion

4.1. Structure of Ru/Al_2O_3 in sol-state

The coordination number and bond length of $RuCl_3$ solution derived from EXAFS shows that the coordination state around Ru atom must greatly depend on the solvents. Namely, the $RuCl_3$ which is dissolved in ethylene glycol solvent, the ethylene glycol and chlorine could be coordinated to form the octahedral structure of Ru complex, whereas the tetrahedral structure of Ru complex could be obtained by the coordination of chlorine atom and water through the hydroxyl bond in aqueous $RuCl_3$ solution.

Lond et al. characterized the coordination state of Ni^{2+} in deuterated ethylene glycol by neutron diffraction. They suggested that ethylene glycol molecules act as bidentate ligands when coordinated to Ni^{2+} in ethylene glycol solution and lead to $Ni(EG)_3^{2+}$ tri-chelate complex [28]. In analogy with those results, considering the coordination number of Ru–O bond in ethylene glycol solution, the ethylene glycol may have bidentate ligands with Ru in solution state. Based on the EXAFS fitting and UV-Vis results of Ru complex, the most probable structure of $RuCl_3$ solution using ethylene glycol or H_2O as solvent is proposed in fig. 10. These structural models suggest that the different structures of Ru complexes are formed depending on the solvents used, and those structural differences may affect the dispersion of Ru particles in alumina matrix after the reduction of catalyst.

From their studies using IR, UV, MAS ^{27}Al-NMR, Tadanaga et al. reported that the structure of aluminum sec-butoxide modified with ethylacetoacetate, which showed that the reaction of acetyl-acetoacetate with aluminum sec-butoxide led to the formation of six-coordinated structural units and aluminum alkoxide formed linear trimer [30]. Livage et al. have studied the exchange reaction between aluminum-sec-butoxide and ethylacetoacetate [40] and proved the bidentate ligand structure by MAS ^{27}Al NMR and FT-IR. In this reaction, the substitution of alkyl groups in highly nucleophilic metal alkoxide can be easily obtained by chemical additives, such as acetylacetoacetate and ethylene glycol containing nucleophilic hydroxyl groups. They formed the bidentate ligand structure through the alcohol-exchange reaction.

In our experiments, the aluminum sec-butoxide is mixed with the solution mixture of $RuCl_3$ and ethylene glycol. The ethylene glycol containing highly nucleophilic hydroxyl group should replace the alkyl group (butoxy group) of Al alkoxide to form the bidentate ethylene glycol–Al ligand structure.

4.2. Ru/Al_2O_3 after gel formation

The role of chelating agent in alkoxide method has been widely reported. As well as occupying a site for condensation, the ethylacetoacetate groups in chelating agent are less susceptible to hydrolysis than the butoxy group, then the chelating agent delays and prevents the complete condensation reaction [12,11]. The chelating

Table 3
Best fit values of the EXAFS spectrum of Ru/Al_2O_3 catalysts calcined and reduced at 500°C [a]

Sample	Back scatterer	N	R (Å)	$\Delta\sigma^2$ (Å^2)
EG-500	Ru	8.4 ± 0.1	2.67 ± 0.01	0.005 ± 10%
W-500	Ru	9.8 ± 0.4	2.68 ± 0.01	0.005 ± 10%
Im-500	Ru	11.4 ± 0.4	2.68 ± 0.01	0.004 ± 10%

[a] N is the coordination number (for the absorber scatter), R is the interatomic distance, and $\Delta\sigma^2$ is the difference between σ^2 values of the sample and the reference.

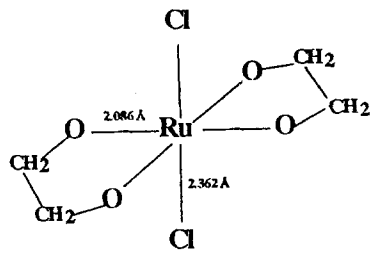

(A)

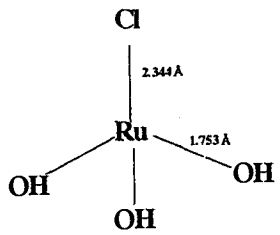

(B)

Fig. 10. Proposed structural model of $RuCl_3$ solution using different solvents based on EXAFS and UV-Vis results. (A) $RuCl_3$ + ethylene glycol and (B) $RuCl_3 + H_2O$.

agent acts as surfactant, and it prevents the agglomeration of aluminum particles in alkoxide sol [11]. Then, the Al_2O_3 gels derived from modified Al_2O_3 have fine and mono dispersed particles.

In our preparation of Ru/Al_2O_3 by the sol–gel method, the ethylene glycol can play an important role to prevent the complete hydrolysis reaction in sol–gel transformation, and also act as surfactant to prevent the agglomeration of Ru/Al_2O_3 particles in the sol-state. The fine and porous Ru/Al_2O_3 with high surface area are obtained after hydrolysis reaction.

In crystallization of Ru/Al_2O_3, the ethylene glycol was an effective modifier to promote the α-phase transition of Ru/Al_2O_3 at low temperatures. Generally, the phase transition of α-Al_2O_3 occurs at ca. 1150–1200°C by nucleation and growth process resulting in a large decrease in surface area [19]. It is reported that the nucleation of α-Al_2O_3 starts from the neck region in which lattice defect and many dislocations are distributed [31]. Based on this principle, several works have been reported to lower the phase transition temperature of α-Al_2O_3 by adding inorganic additives such as Fe_2O_3 and α-Al_2O_3 [32]. Mizukami et al. reported the particle size and crystallization of Al_2O_3 prepared by sol–gel method with organic additives. They greatly depended on the complexing abilities of the solvents, and strong complexing agents like polyethylene glycol and branched diol yield an alumina crystallizing to α-phase at lower temperatures [15]. In our results, ethylene glycol had strong chelating ability in the starting solution state and formed a stable bidentate ligand structure with Ru and Al. This stable bidentate structure not only helped to promote the α-phase transition at low temperatures but also assisted to prevent the sintering of Ru/Al_2O_3, which led to high surface area at high temperature calcination. In addition, the phase transition to the thermally stable α-Al_2O_3 phase can be promoted by the bidentate coordination of ethylene glycol to aluminum atom. This site can make a large amount of defects during the calcination in air atmosphere and the high concentration of defects promotes the structural rearrangement of alumina gel to make a stable phase, of α-Al_2O_3, at 800°C. In TiO_2 system, we also observed rutile phase transition at low temperature (300°C) by the bidentate organic additives in the sol–gel process [16]. The phase transition mechanism of α-Al_2O_3 should be analogous to that of rutile phase in TiO_2 system.

The EXAFS spectra of Ru/Al_2O_3 calcined at 300°C showed the smaller ruthenium oxide particles were formed in EG-300 compared with W-300 catalyst. It is well known that Ru atom begins to migrate mainly under severe oxidation atmosphere (> 250°C). In our previous study, the size of Ru is greatly affected by treatment conditions, which could be characterized by ^{129}Xe-NMR, ^{129}Xe-adsorption, and TEM [39]. In our Ru/Al_2O_3 catalyst prepared by the sol–gel method, the stable bidentate Ru complex is formed in using ethylene glycol solution, and this stable Ru structure in alumina matrix was maintained up to 200°C calcination. This enhanced stability must be effective to prevent the migration of Ru particles under oxidation conditions (> 300 or 500°C) because the migration of atomic ruthenium should start from 200–300°C. By contrast, in W-sol after gel formation, the ruthenium oxide (Ru–O–Ru) bond was suggested from the EXAFS spectra. It implied that the oxidation of Ru could be easily progressed in the presence of ruthenium oxide bond and big particles of ruthenium oxide might be obtained after calcination in air atmosphere (300–500°C) due to the easy formation of ruthenium oxide species below 300°C. After hydrogen reduction at 500°C, the small ruthenium metal was obtained in EG-500 catalysts compared with other catalysts. It is known that the oxidation species and its size have strong effect on the size of metal in Pt/Al_2O_3 and Co/TiO_2 catalysts [21]. Similarly, the formation of small ruthenium oxide under oxidation condition is strongly related to the final size of ruthenium metal after hydrogen reduction at 500°C. The enhanced thermal stability of Ru complex by the addition of ethylene glycol must be effective to form small Ru oxide under air calcination. As a result, ethylene glycol modified Ru and Al structures at the initial solution should be critical to control the particle size of Ru after the reduction as well as the phase of alumina support.

5. Conclusion

Depending on the solvents (ethylene glycol or H_2O) in the sol–gel process, different initial structures of Ru complexes are suggested, and these structural differences in solution state affect the final dispersion of Ru in alumina matrix. Ethylene glycol was effective to prepare the Ru/Al_2O_3 catalyst with thermally stable alumina of high surface area. The ethylene glycol coordinated to Ru as well as Al ion in the initial stage and proved to be important to control the final properties of the Ru/Al_2O_3 catalyst.

Acknowledgement

This work was financially supported by the Yukong Corporation Inc. The authors thank KEK (National Laboratory for High Energy Physics, Japan) for EXAFS measurements and Dr. Ryong Ryoo for ^{13}C-NMR measurements.

References

[1] M.A. Vannice, J. Catal. 37 (1975) 449.
[2] J.H. Sinfelt, in: *Bimetallic Catalysts: Discoveries, Concepts, and Applications* (Wiley, New York, 1983).
[3] R.D. Gonzalez and H. Miura, J. Catal. 77 (1982) 338.
[4] B. Delmon and P.A. Jacobs, in: *Preparation of Catalysts I* (Elsevier, Amsterdam, 1975).
[5] C.J. Brinker and G.W. Scherer, in: *Sol–Gel Science: The Physics and Chemistry of Sol–Gel Processing* (Academic Press, San Diego, 1990).
[6] T. Lopez, A. Lopez-Gaona and R. Gomez, J. Non-Cryst. Solids 110 (1989) 170.
[7] T. Lopez, R. Gomez, O. Novaro, A. Ramirez-Solis, E. Sanchez-Mora, S. Castillo, E. Poulain and J.M. Martinez-Magadan, J. Catal. 141 (1993) 114.
[8] T. Lopez, P. Bosch, M. Asomoza, and R. Gomez, J. Catal. 133 (1992) 247.
[9] T. Lopez, M. Asomoza, P. Bosch, E. Garcia-Gigueroa and R. Gomez, J. Catal. 138 (1992) 463.
[10] K. Balakrishnan and R.D. Gonzalez, J. Catal. 144 (1993) 395.
[11] C. Sanchez, J. Livage, M. Henry and F. Babonneau, J. Non-Cryst. Solids 100 (1988) 65.
[12] R. Nass and H. Schmidt, J. Non-Cryst. Solids 121 (1990) 329.
[13] M. Inoue, H. Kominami and T. Inui, J. Chem. Soc. Dalton Trans. (1991) 3331.
[14] M. Inoue, H. Kominami and T. Inui, J. Am. Ceram. Soc. 75 (1992) 2597.
[15] K. Maeda, F. Mizukami, S. Niwa, M. Toba, M. Watanabe and K. Masuda, J. Chem. Soc. Faraday Trans. 88 (1992) 97.
[16] K. Oh, J.C. Yang, K.T. Jung and Y.G. Shul, KJChe, to be published.
[17] F.M. Nelson and F.T. Eggertsen, Anal. Chem. 30 (1958) 1387.
[18] B.K. Teo, in: *EXAFS: Basic Principles and Data Analysis* (Springer, Berlin, 1986).
[19] W.H. Critzen, ed., in: *Alumina as a Ceramic Material* (American Ceramic Society, Columbus, 1970)
[20] M. Inoguchi, K. Tate, Y. Kaneko, Y. Satomi, K. Inaba, T. Mizutori, H. Kagaya, R. Nishiyama, S. Onishi and T. Nagai, Bull. Jpn. Petrol. Inst. 13 (1975) 289.
[21] K. Tohji, Y. Udagawa, S. Tanabe and A. Ueno, J. Am. Chem. Soc. 106 (1984) 612.
[22] K. Asakura and Y. Iwasawa, J. Chem. Soc. Faraday Trans. 86 (1990) 2657.
[23] K. Asakura, K. Bando and Y. Iwasawa, J. Chem. Soc. Faraday Trans. 86 (1990) 2645.
[24] C. Jorgensen, Acta Chem. Scand. 10 (1956) 518.
[25] Z. Harzion and G. Navon, Inorg. Chem. 19 (1980) 2237.
[26] M. Vaarkamp, F. Modica, J. Miller and D. Koningsberger, J. Catal. 144 (1993) 611.
[27] H. Sakane, T. Miyanaga, I. Watanabe and Y. Yokoyama, Chem. Lett. (1990) 1623.
[28] P. Lond, P. Salmon and D. Champeney, J. Am. Chem. Soc. 113 (1991) 6420.
[29] K. Tohji, Y. Udagawa, S. Tanabe, T. Ida and A. Ueno, J. Am. Chem. Soc. 106 (1984) 5172.
[30] K. Tadanaga, T. Iwami, N. Tohge and T. Minami, J. Sol–Gel Sci. Technol. 3 (1994) 5.
[31] H. Schaper, E.B.M. Doesburg, P.H.M. de Korte and L. Reijen, Solid State Ionics 16 (1985) 261.
[32] R. Shelleman, G. Messing and M. Kumagai, J. Non-Cryst. Solids 82 (1986) 277.
[33] K. Maeda, F. Mizukami, M. Watanabe, N. Arai, S. Niwa, M. Toba and K. Shimizu, J. Mater. Sci. Lett. 9 (1990) 522.
[34] F. Mizukami, K. Maeda, M. Watanabe, K. Masuda, T. Sano and K. Kuno, in: *Catalysis and Automotive Pollution Control II*, ed. A. Crucq. (Elsevier, Amsterdam, 1990).
[35] A.F. Wells, in: *Structural Inorganic Chemistry*, 5th Ed. (Clarendon Press, Oxford, 1984).
[36] F. Lytle, G. Via and H. Sinfelt, J. Chem. Phys. 67 (1977) 3831.
[37] C. Macgillavry, in: *International Tables for X-ray Crystallography*, Vol. III, eds. C. Macgillavry, G. Rieck and K. Lonsdale (Reidel, Dordrecht, 1983).
[38] M. Miyake, N. Nakagawa, H. Ohyanagi and T. Suzuki, Inorg. Chem. 25 (1986) 700.
[39] S.J. Cho, S.M. Jung, Y.G. Shul and R. Ryoo, J. Phys. Chem. 96 (1992) 9922.
[40] L. Bonhomme-Coury, F. Babonneau and J. Livage, J. Sol–Gel Sci. Technol. 3 (1994) 157.